

Femtosecond laser pulse energy transfer induced by plasma grating due to filament interaction in air

Xuan Yang, Jian Wu, Yuqi Tong, Liang'en Ding, Zhizhan Xu, and Heping Zeng^{a)}
*State Key Laboratory of Precision Spectroscopy, East China Normal University, Shanghai 200062,
 People's Republic of China*

(Received 3 January 2010; accepted 20 July 2010; published online 17 August 2010)

We experimentally demonstrate the formation of a thin plasma grating lasted for several tens of picosecond induced by the strong interaction between two noncollinear femtosecond filaments in air. A time-delayed second-harmonic pulse propagating along one of the incident filaments is coupled and nonlinearly diffracted by the thin plasma grating, leading to an energy transfer to the other noncollinearly crossed femtosecond filament. The dependences of the plasma grating on the intensity ratios and relative polarizations between the input pulses are investigated. © 2010 American Institute of Physics. [doi:10.1063/1.3479499]

Self-guided propagation of ultrashort intense laser pulses in air has been extensively studied as a fundamental phenomenon with abundant self-action nonlinearities such as pulse self-compression,¹ energy reservoir,² and for the use in a variety of applications including supercontinuum generation,³ lightning and discharge triggering,⁴ remote-sensing,⁵ and terahertz (THz) emission.⁶ It has been recently demonstrated that the filament interaction in molecular gases could be controlled by using molecular alignment.^{7–10} In addition, multifilament interaction was demonstrated to induce significant THz enhancement¹¹ and two-beam coupling.¹²

For filaments¹³ of noncollinear interaction, the plasma density generated in the interaction region is modulated due to the interference between filaments. It could create a volume of plasma with periodic wavelength-scale microstructures, which are analogous to grating or photonic lattices.^{14,15} In this work, we experimentally demonstrated that a thin plasma grating could be created via strong interaction between two noncollinear fs filaments crossed at angles of few degrees in air. Based on the second-order diffraction from the plasma grating, energy transfer of a time-delayed second-harmonic (SH) pulse from one of the incident fundamental-wave (FW) filaments to the other one was observed. Since the plasma density modulation changed with the intensity ratios and relative polarizations between the incident FW filaments, the diffraction efficiency of the SH pulse varied accordingly.

The experimental setup is schematically shown in Fig. 1(a). A 2.2 mJ, 45 fs pulse at 800 nm from a Ti:sapphire amplifier laser system was equally split into two parts as the pump and probe pulses, respectively. In the pump arm, a 0.5 mm thick BBO crystal was used to produce a SH pulse at 400 nm. The generated SH pulse was separated from the FW pulse with a dichroic mirror (HR@400/AR@800 nm) and passed through a motorized translation stage, which was then combined collinearly with the FW pulse by another dichroic mirror. In the probe arm, a half-wave plate and a neutral density attenuator were inserted to control its relative pulse energy and field polarization. By using two lens of

$f=100$ cm, both the pump and probe pulses were focused to produce two noncollinear filaments in air at a crossing angle variable from 2° to 4° . The length of each individual filament was measured to be ~ 5 cm. The polarization of the SH pulse was orthogonal to that of the FW pulse. At the end of the filament interaction, for both the pump and probe beams, the SH pulses were separated from the incident FW pulses with dichroic mirrors and then sent to the photodetectors for the energy transfer analysis. A lock-in amplifier was used in the measurements to improve the signal-to-noise ratio.

For noncollinear filament interaction in air, when the high-intensity pump and probe pulses are temporally overlapped, wavelength-scale periodic lattice of plasma microstructures are created and projected along a relatively long distance by means of filamentation in periodically localized regions, where parallel plasma self-channels are formed around the optical field interference peaks due to the spatially localized counterbalance among self-focusing, plasma defocusing, and higher-order nonlinear effects. Based on the plasma density modulation in the interaction region, the reflective index proportional to $n=n_0-\rho(r,t)/\rho_c$ changes periodically due to the multiphoton ionization induced plasma density $\rho(r,t)$, where ρ_c denotes the critical plasma density. As a result, a plasma grating persisted several tens of picosecond is formed, whose period is given by $\lambda/[2 \sin(\theta/2)]$, where λ is the central wavelength and θ is the crossing angle of the noncollinear input pulses. In order to clearly demonstrate the existence of plasma grating, the fluorescence generated from nitrogen molecular ions inside the interaction region was measured with the same instrument as described in Ref. 14. The results are shown in the inset of Fig. 1(a). The periodic distribution in the overlapped region fully justified the existence of plasma grating induced by filament interaction. Here, the spatial period of plasma grating was measured to be $\Lambda \sim 16.1 \mu\text{m}$ at a crossing angle of 3° , which agreed with the value of $\Lambda \sim 15.3 \mu\text{m}$ determined by $\lambda/[2 \sin(\theta/2)]$. Figure 1(b) shows the measured plasma grating as the relative intensity and field polarization between the pump and probe pulses were changed, which clearly indicates the strong dependences of the induced plasma grating on the incident FW pulses. According to the measurement of N_2 fluorescence as shown in the Fig. 1, we could derive that the plasma grating exhibited the typical characteristics of a thin

^{a)}Author to whom correspondence should be addressed. Electronic mail: hpzeng@phy.ecnu.edu.cn.

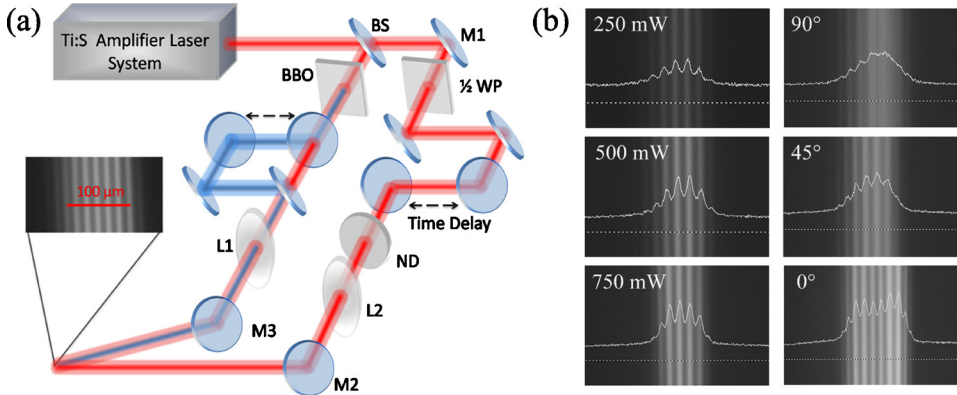


FIG. 1. (Color online) (a) The scheme of the experimental setup, and (b) the dependence of the plasma grating on the field polarization and incident energy of the probe pulse. BS: beam splitter; 1/2 WP: half-wave plate; ND: adjustable neutral attenuator; L1 and L2: lens.

grating. The effective thickness of the plasma grating was estimated to be $D \sim 100 \mu\text{m}$ from the measured spatial distribution of N_2 fluoresce in the filament interaction region, and we thus reached the parameter $\gamma = D/\Lambda \sim 6$ (smaller than 10), indicating a thin plasma grating generated by the non-collinear filament interaction.

Interestingly, accompanied with the FW filament interaction, an efficient energy transfer of a time-delayed SH pulse from the pump filament to the probe one was observed. Figure 2 shows the photographs of the pump and probe beams with and without filament interaction taken with a digital camera on an observation screen placed at a distance of 1 m after the filament crossing point. There were no SH pulses in the probe beam when the pump (right) and probe (left) pulses were temporally separated each other as shown in Fig. 2(a). As the pump and probe pulses were adjusted to be temporally overlapped, a bright blue spot appeared at the propagation direction of the probe beam, and a weak one appeared at the bisector of the pump and probe propagation directions. For the thin plasma grating, the diffraction of the time-delayed SH pulse is governed by $\Lambda[\sin(\alpha + \varphi_m) - \sin(\alpha)] = m\lambda_d$, $m = 0, \pm 1, \pm 2, \dots$, where α and φ_m denote the angle of incidence and diffraction beams, respectively, λ_d is the wavelength of the SH light wave, and Λ is the spatial period of the grating determined by $\lambda/[2 \sin(\theta/2)]$.¹⁶ In our experiment, for sufficiently small angles α and φ_m , the angle of m th order of diffraction was given by $\varphi_m = m\lambda/\Lambda$. Under these conditions, for the SH pulse incidence along the pump arm, the first and second order diffraction angles were $\varphi_1 = \theta/2$ and $\varphi_2 = \theta$, respectively, corresponding to the bisector of the pump and probe beams and the probe beam direction, which agreed with our experimental observation as shown in Fig. 2(b). Note that the SH energy of the first-order diffraction was less than that of the second-order diffraction, which was caused by the amplitude-dependent phase change of the thin phase grating.¹⁷ However, in our experiment, the SH appeared in the bisector of the pump and probe beams was not only originated from the first-order diffraction of SH but

also from the SH guided in the plasma waveguide array¹⁴ due to refractive index distribution in the interaction region, wherein the incident and diffracted SH pulses were guided in these channels. It was different from the case of a standard phase thin grating.

We next checked the diffraction efficiency during the filament interaction with different incident SH pulse energies. For a non-collinear crossing angle of 3° , the SH energies coupled to the probe arm were measured to be 5 and $1 \mu\text{J}$ at the incident SH pulse energies of 220 and $80 \mu\text{J}$ along the pump beam, corresponding to the energy transfer efficiency of 2.3% and 1.25%, respectively. The increase in the energy transfer efficiency with the incident SH energy indicated that the observed SH along the probe beam was caused by nonlinear rather than linear diffraction. This could be attributed to the interference between the incident and diffracted SH pulses that altered the thin plasma grating. As the incident and diffracted SH pulses were coupled to the thin plasma waveguide at exactly the same angles of the pump and probe directions, their interference enhanced plasma density modulation in the overlapped region at high-peak-intensity incidence. As a result, the SH diffraction efficiency varied nonlinearly with the incident SH energy, leading to the observed energy transfer equivalent to two-beam coupling rather than a mere diffraction of the incident SH pulses. As the thin plasma grating was more sensitive to the

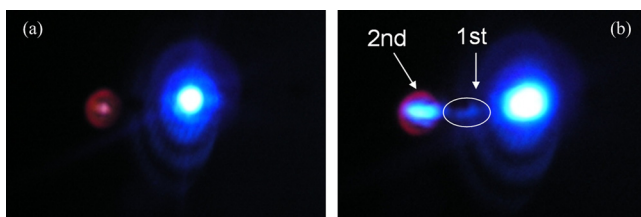


FIG. 2. (Color online) Far-field images of the pump and probe beams when the filament interaction was turned (a) off and (b) on.

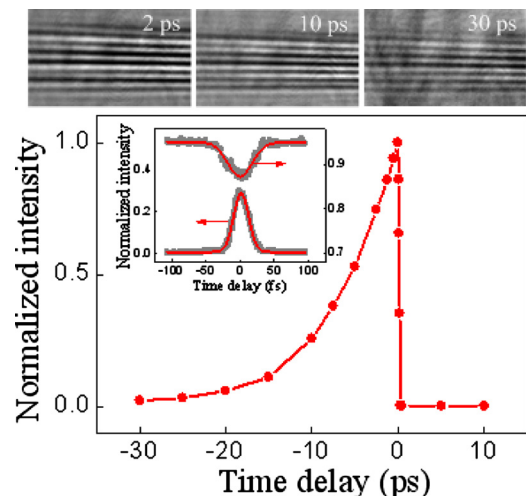


FIG. 3. (Color online) The measured relative intensity of the SH pulse in the probe arm as a function of the delay of the SH pulse with respect to the FW pulses. Inset: the plasma grating at different time delay; SH signal in the pump (upper) and probe (bottom) arms, respectively, varied as the delay between pump and probe pulses for a fixed SH pulse delay of -100 fs .

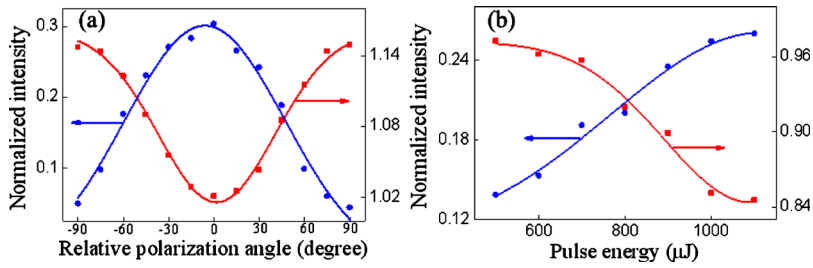


FIG. 4. (Color online) The measured dependences of the SH pulse intensity in pump (red square) and probe (blue circle) beams on (a) the relative field polarization and (b) the pulse energy of the probe pulse.

incident SH pulses than the thick grating,¹⁵ nonlinear diffraction could be more easily observed for the case of the thin plasma grating.

We also checked the dependence of the transferred SH beam along the probe beam upon the time delay of the SH probe pulse with respect to the FW pulses. As shown in Fig. 3, only for the SH pulse arrived after the plasma grating formation (negative delays) could the diffracted signal be detected along the probe beam, and the diffracted signal decreased gradually as the SH pulse delayed further, implying that the plasma density modulation within the plasma grating was reduced gradually after the plasma grating formation. The upper inset in Fig. 3 shows the image of plasma grating at different delays between the SH and FW pulses. The maximum plasma density modulation reached at zero delay when the FW filament interaction was launched, after which the plasma grating was gradually decayed and consequently disappeared. In our experiment, the plasma grating could last for about ~ 30 ps. No SH pulses were observed along the probe beam as the SH pulse passed through the overlapped region before the grating was formed (positive delay), since no diffraction was possible in this range of delay. The inset shows the relative SH pulse energy along the pump and probe beams recorded by tuning the pump-probe delay at a fixed SH pulse delay of -100 fs. A clear change in the SH energy was observed only when the pump and probe pulses were synchronized. This confirmed that the plasma grating was formed by the noncollinear filament interaction with a lifetime of several tens of picosecond.

We then investigated the change in the energy transfer efficiency of the SH pulse by varying the intensity and field polarization of the probe pulse while the pump pulse was horizontally polarized with a fixed pulse energy of 1.1 mJ. Figure 4(a) shows the measured relative intensity of the SH pulses along the pump (red curve) and probe (blue curve) beams when the field polarization of the probe pulse was rotated. The SH pulse along the probe beam got the maximum and minimum as the probe polarization was, respectively, parallel and orthogonal to the pump polarization, corresponding to the cases with and without plasma grating in the overlapped region, respectively. While the SH pulse along the pump beam showed the opposite trend as the relative polarization was changed. In addition, the plasma grating was critically dependent on the relative intensity ratio ($P_{\text{probe}}/P_{\text{pump}}$) since the interference modulation depth changed at different intensity ratios. Accordingly, the SH energy transfer efficiency changed with the probe intensity, as shown in Fig. 4(b). The energy transfer of the SH pulse from the pump to the probe beam got its maximum with a unity

intensity ratio between the pump and probe pulses, corresponding to a maximum modulation depth of the formed plasma grating, which was consistent with our previous observations on enhanced third-harmonic generation by filament interaction.¹¹

In summary, energy transfer of a delayed SH pulse from one FW beam to the other one was observed due to the coupling and diffraction of the plasma grating formed by the strong interaction between two noncollinear fs filaments in air. The results are promising for some important applications in studying laser-plasma interactions and high-intensity ultrafast phenomena with all-optical-induced plasma beam couplers.

This work was partly funded by National Natural Science Fund (Grant Nos. 10525416 and 10804032) and National Key Project for Basic Research (Grant No. 2006CB806005).

¹A. Couairon, M. Franco, A. Mysyrowicz, J. Biegert, and U. Keller, *Opt. Lett.* **30**, 2657 (2005).

²M. Mlejnek, M. Kolesik, J. V. Moloney, and E. M. Wright, *Phys. Rev. Lett.* **83**, 2938 (1999).

³J. Yu, D. Mondelain, G. Ange, R. Volk, S. Niedermeier, J. P. Wolf, J. Kasparian, and R. Sauerbrey, *Opt. Lett.* **26**, 533 (2001).

⁴J. Kasparian, R. Ackermann, Y.-B. André, G. Méchain, G. Méjean, B. Prade, P. Rohwetter, E. Salmon, K. Stelmasczyk, J. Yu, A. Mysyrowicz, R. Sauerbrey, L. Woeste, and J.-P. Wolf, *Opt. Express* **16**, 5757 (2008).

⁵H. Rairoux, S. Schillinger, M. Niedermeier, F. Rodriguez, R. Ronneberger, B. Sauerbrey, D. Stein, C. Waite, H. Wedekind, L. Wille, C. Wöste, and C. Ziener, *Appl. Phys. B: Lasers Opt.* **71**, 573 (2000).

⁶C. D'Amico, A. Houard, M. Franco, B. Prade, A. Mysyrowicz, A. Couairon, and V. T. Tikhonchuk, *Phys. Rev. Lett.* **98**, 235002 (2007).

⁷S. Varma, Y.-H. Chen, and H. M. Milchberg, *Phys. Rev. Lett.* **101**, 205001 (2008).

⁸H. Cai, J. Wu, H. Li, X. S. Bai, and H. P. Zeng, *Opt. Express* **17**, 21060 (2009).

⁹J. Wu, H. Cai, P. F. Lu, X. S. Bai, L. E. Ding, and H. P. Zeng, *Appl. Phys. Lett.* **95**, 221502 (2009).

¹⁰R. Bartels, T. Weinacht, N. Wagner, M. Baertschy, C. Greene, M. Murnane, and H. Kapteyn, *Phys. Rev. Lett.* **88**, 013903 (2001).

¹¹X. Yang, J. Wu, Y. Peng, Y. Q. Tong, S. Yuan, L. E. Ding, Z. Z. Xu, and H. P. Zeng, *Appl. Phys. Lett.* **95**, 111103 (2009).

¹²A. C. Bernstein, M. McCormick, G. M. Dyer, J. C. Sanders, and T. Ditmire, *Phys. Rev. Lett.* **102**, 123902 (2009).

¹³A. Couairon and A. Mysyrowicz, *Phys. Rep.* **441**, 47 (2007).

¹⁴X. Yang, J. Wu, Y. Peng, Y. Q. Tong, P. F. Lu, L. E. Ding, Z. Z. Xu, and H. P. Zeng, *Opt. Lett.* **34**, 3806 (2009).

¹⁵S. Suntsov, D. Abdollahpour, D. G. Papazoglou, and S. Tzortzakis, *Appl. Phys. Lett.* **94**, 251104 (2009).

¹⁶H. J. Eichler and A. Hermerschmidt, *Photorefractive Materials and Their Applications* (Springer, New York, 2006), Vol. 1, pp. 7–42.

¹⁷J. W. Goodman, *Introduction to Fourier Optics* (McGraw-Hill, New York, 1996).